

## Synthesis and Properties of the Negative Thermal Expansion Material Cubic ZrMo<sub>2</sub>O<sub>8</sub>

Cora Lind,<sup>†</sup> Angus P. Wilkinson,<sup>\*,†</sup> Zhongbo Hu,<sup>‡</sup> Simine Short,<sup>§</sup> and James D. Jorgensen<sup>§</sup>

*School of Chemistry and Biochemistry, Georgia Institute of Technology, Atlanta, GA 30332-0400, and Materials Science Division and Intense Pulsed Neutron Source Division, Argonne National Laboratory, Argonne, IL 60439*

Received June 22, 1998

Revised Manuscript Received August 5, 1998

Materials that exhibit negative thermal expansion are of considerable scientific and technological interest.<sup>1–3</sup> Their use in composites can facilitate the control of bulk thermal expansion properties to obtain a good match to other system components or zero expansion. Zero, or close to zero, thermal expansion is needed for various applications in optics, electronics, and other fields where exact positioning of parts is crucial. Nearly all materials that undergo negative thermal expansion display this property over a narrow temperature range or show anisotropic expansion behavior that can lead to microcracks. Recently, isotropic negative thermal expansion over the temperature range 0.3–1050 K has been reported for cubic ZrW<sub>2</sub>O<sub>8</sub><sup>4,5</sup> along with studies of its behavior under pressure.<sup>6,7</sup> The structural similarity of many tungsten and molybdenum compounds strongly suggested the possibility of a cubic ZrMo<sub>2</sub>O<sub>8</sub> with related properties. Sleight and co-workers have recently prepared compositions in the solid solution ZrW<sub>2-x</sub>Mo<sub>x</sub>O<sub>8</sub>, although they have been unable to make samples with  $x > 1.5$ .<sup>3</sup> Here we report the first preparation and characterization of the end member cubic ZrMo<sub>2</sub>O<sub>8</sub>.

Zirconium molybdates and basic zirconium molybdate hydrates have been investigated as acid and oxidation catalysts,<sup>8</sup> ion-exchangers,<sup>9</sup> luminescent materials,<sup>10</sup> fission products in nuclear fuel,<sup>11</sup> and byproducts in nuclear fuel reprocessing.<sup>12</sup> However, only trigonal<sup>13–15</sup>

and monoclinic<sup>14,16</sup> forms of ZrMo<sub>2</sub>O<sub>8</sub> had been reported, suggesting that cubic ZrMo<sub>2</sub>O<sub>8</sub>, if it could be prepared, would only exist as a metastable material. Our experience with the low temperature (~650 °C) synthesis of pure cubic ZrW<sub>2</sub>O<sub>8</sub> by the dehydration of ZrW<sub>2</sub>O<sub>7</sub>(OH/Cl)<sub>2</sub>·2H<sub>2</sub>O<sup>18</sup> combined with literature on the preparation of HfW<sub>2</sub>O<sub>8</sub><sup>17</sup> and a comment by Clearfield and Blessing,<sup>9</sup> regarding an unidentified, possibly metastable, phase formed upon heating ZrMo<sub>2</sub>O<sub>7</sub>(OH)<sub>2</sub>·2H<sub>2</sub>O, led us to attempt the low-temperature preparation of cubic ZrMo<sub>2</sub>O<sub>8</sub>.

Zirconium molybdenum oxide hydroxide hydrate (ZrMo<sub>2</sub>O<sub>7</sub>(OH)<sub>2</sub>·2H<sub>2</sub>O)<sup>9</sup> was dehydrated by heating to 365 °C at 4°/min, holding at this temperature for 13.5 h, and heating further to 390 °C for 5–15 min. The product obtained on rapid cooling to room temperature, cubic ZrMo<sub>2</sub>O<sub>8</sub>, has an X-ray diffraction pattern that is very similar to that of ZrW<sub>2</sub>O<sub>8</sub>. A comparison of the calculated pattern for cubic ZrMo<sub>2</sub>O<sub>8</sub>, assuming a β-ZrW<sub>2</sub>O<sub>8</sub> structure, with the observed X-ray data is presented in Figure 1. The presence of trigonal ZrMo<sub>2</sub>O<sub>8</sub> in trace amounts is apparent from this figure. Other heating times and temperatures led to an as yet unidentified dehydrated phase which forms at about 150 °C, trigonal ZrMo<sub>2</sub>O<sub>8</sub>, or mixtures of these three phases. A similar procedure was also used to prepare HfMo<sub>2</sub>O<sub>8</sub> and a variety of solid solutions of formula Hf<sub>x</sub>Zr<sub>1-x</sub>W<sub>y</sub>Mo<sub>2-y</sub>O<sub>8</sub> with 0 ≤  $x$  ≤ 1 and 0 ≤  $y$  ≤ 2. The temperature required to obtain the pure cubic phase varies with composition. Freshly prepared cubic ZrMo<sub>2</sub>O<sub>8</sub> was examined by SEM and found to contain rodlike aggregates with dimensions 5–10 μm. Each aggregate was made up of submicron rodlike crystallites.

The thermal expansion of cubic ZrMo<sub>2</sub>O<sub>8</sub> was investigated using both variable temperature X-ray and neutron diffraction. Neutron diffraction data were collected using the special environment powder diffractometer (SEPD)<sup>19</sup> at the Intense Pulsed Neutron Source, Argonne National Laboratory, in a Displex refrigerator between 11 K and room temperature and in a furnace between room temperature and 573 K. X-ray data were collected between 298 and 573 K on a Scintag X1-diffractometer equipped with a Scintag variable temperature sample stage. For all of the X-ray measurements, NIST SRM 660 LaB<sub>6</sub> or NIST SRM 640b Si was used as an internal standard. The diffraction data were analyzed by the Rietveld method using GSAS.<sup>20</sup> Lattice constants for cubic ZrMo<sub>2</sub>O<sub>8</sub> were obtained from the

<sup>†</sup> Georgia Institute of Technology.

<sup>‡</sup> Intense Pulsed Neutron Source Division, Argonne National Laboratory.

<sup>§</sup> Materials Science Division, Argonne National Laboratory.

(1) Roy, R.; Agrawal, D. K.; McKinstry, H. A. *Annu. Rev. Mater. Sci.* **1989**, *19*, 59–81.

(2) Sleight, A. W. *Endeavour* **1995**, *19*, 64–68.

(3) Sleight, A. W. *Inorg. Chem.* **1998**, *37*, 2854–2860.

(4) Mary, T. A.; Evans, J. S. O.; Vogt, T.; Sleight, A. W. *Science* **1996**, *272*, 90–92.

(5) Evans, J. S. O.; Mary, T. A.; Vogt, T.; Subramanian, M. A.; Sleight, A. W. *Chem. Mater.* **1996**, *8*, 2809–2823.

(6) Evans, J. S. O.; Hu, Z.; Jorgensen, J. D.; Argyriou, D. N.; Short, S.; Sleight, A. W. *Science* **1997**, *275*, 61–65.

(7) Perottoni, C. A.; de Jornada, J. A. H. *Science* **1998**, *280*, 886–889.

(8) Prinetto, F.; Cerrato, G.; Ghiotti, G.; Chiorino, A.; Campa, M. C.; Gazzoli, D.; Indovina, V. *J. Phys. Chem.* **1995**, *99*, 5556–5567.

(9) Clearfield, A.; Blessing, R. H. *J. Inorg. Nucl. Chem.* **1972**, *34*, 2643–2663.

(10) Blasse, G.; Dirksen, G. J. *J. Phys. Chem. Solids* **1987**, *48*, 591–592.

(11) Pankajavalli, R.; Sreedharan, O. M. *J. Nucl. Mater.* **1990**, *172*, 151–154.

(12) Adachi, T.; Muromura, T.; Takeshi, H.; Yamamoto, T. *J. Nucl. Mater.* **1988**, *160*, 81–87.

(13) Auray, M.; Quarton, M.; Tarte, P. *Acta Crystallogr.* **1986**, *C42*, 257–259.

(14) Auray, M.; Quarton, M.; Tarte, P. *Powder Diffr.* **1987**, *2*, 36–38.

(15) Serezhkin, V. N.; Efremov, V. A.; Trunov, V. K. *Russ. J. Inorg. Chem.* **1987**, *32*, 1566–1570.

(16) Auray, M.; Quarton, M. *Powder Diffr.* **1989**, *4*, 29–30.

(17) Palitsyna, S. S.; Mokhosoev, M. V.; Krivobok, V. I. *Bull. Acad. Sci. USSR, Div. Chem. Sci.* **1977**, 611–613.

(18) Dadachov, M. S.; Lambrecht, R. M. *J. Mater. Chem.* **1997**, *7*, 1867–1870.

(19) Jorgensen, J. D.; Faber, J., Jr.; Carpenter, J. M.; Crawford, R. K.; Haumann, J. R.; Hittman, R. L.; Kleb, R.; Ostrowski, G. E.; Rotella, F. J.; Worlton, T. G. *J. App. Crystallogr.* **1989**, *22*, 321–333.

(20) Larson, A. C.; Von Dreele, R. B. *GSAS—General Structure Analysis System*; Report LA-UR-86-748: Los Alamos Laboratory, 1987.

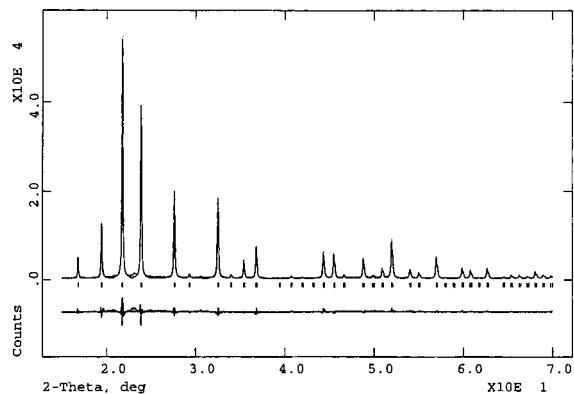


**Figure 1.** A comparison of the room-temperature powder X-ray diffraction pattern for cubic  $\text{ZrMo}_2\text{O}_8$  with that calculated by Rietveld refinement assuming a  $\beta\text{-ZrW}_2\text{O}_8$  structural model. The calculated reflection positions are indicated by tick marks and the difference between the observed and calculated patterns is also shown. Peaks from trace amounts of trigonal  $\text{ZrMo}_2\text{O}_8$  can be seen in the region  $20\text{--}25^\circ 2\theta$  and at approximately  $31^\circ 2\theta$ .

X-ray diffraction data by fixing the lattice parameter of the internal reference material at the certified value after correction for thermal expansion<sup>21</sup> and refining the lattice constant for cubic  $\text{ZrMo}_2\text{O}_8$  along with sample height and zero point correction terms. The required diffractometer constants for the analysis of the neutron diffraction data were obtained by fitting them to the room-temperature data measured in both the Displex refrigerator and the furnace while fixing the  $\text{ZrMo}_2\text{O}_8$  lattice constant at the value determined using X-ray diffraction at room temperature. These diffractometer constants were then used for the analysis of the neutron diffraction data obtained at other temperatures. Neutron diffraction data were also collected over the pressure range 0–0.6 GPa at room temperature in a cell pressurized with helium.<sup>22</sup> Lattice constants were obtained from these data by Rietveld analysis.

The lattice constant of cubic  $\text{ZrMo}_2\text{O}_8$  at 298 K was determined to be  $a = 9.1304(2)$  Å by averaging the values obtained from six independent X-ray data sets. Cubic  $\text{ZrMo}_2\text{O}_8$  is thermodynamically metastable; it crystallizes in a temperature range that is also compatible with the formation of trigonal  $\text{ZrMo}_2\text{O}_8$ , to which it is converted completely upon long holding times at  $\sim 390^\circ\text{C}$  or by heating to higher temperatures. The conversion of cubic  $\text{ZrMo}_2\text{O}_8$  to the trigonal phase is sensitive to the exact conditions used to prepare the cubic phase. The formation of trigonal  $\text{ZrMo}_2\text{O}_8$  from the cubic phase, rather than the thermodynamically more stable monoclinic phase, indicates that the outcome of the transformation process is kinetically controlled.

Cubic  $\text{ZrW}_2\text{O}_8$  is reported to adopt an ordered structure ( $\alpha\text{-ZrW}_2\text{O}_8$ , space group  $P2_13$ ) below 428 K and to transform to a disordered centrosymmetric form at higher temperatures ( $\beta\text{-ZrW}_2\text{O}_8$ , space group  $Pa\bar{3}$ ).<sup>4,5</sup> This results in a discontinuity in the thermal expansion for the material;  $\alpha \sim -4.9 \times 10^{-6} \text{ K}^{-1}$  (430–950 K) and  $\alpha \sim -8.8 \times 10^{-6} \text{ K}^{-1}$  (0–400 K). Our neutron and X-ray

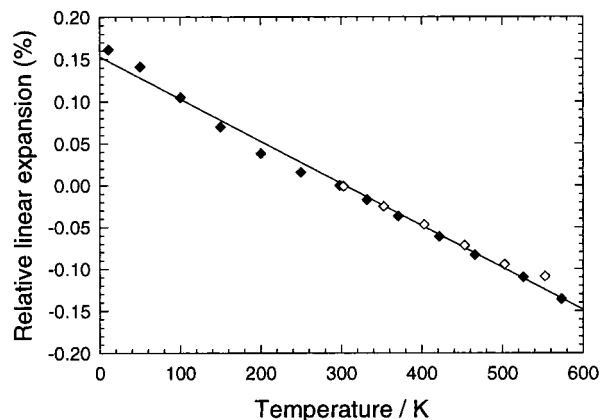


**Figure 2.** Relative thermal expansion for cubic  $\text{ZrMo}_2\text{O}_8$  (defined as  $100 \times [a_T - a_{298}]/a_{298}$ ). The solid and open diamonds were determined from neutron and X-ray diffraction data, respectively. The straight line is a best fit to all of the data points, giving an average linear thermal expansion coefficient of  $-5.0 \times 10^{-6} \text{ K}^{-1}$ .

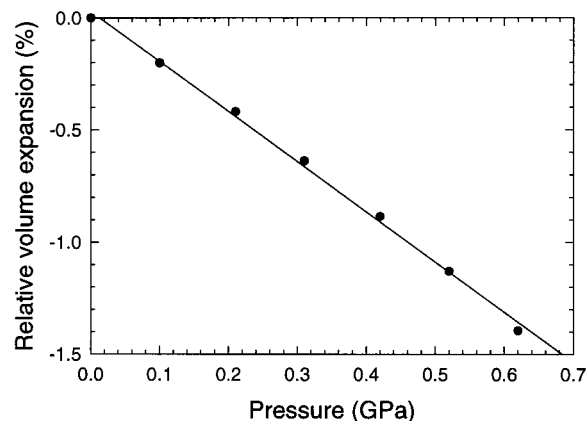


**Figure 3.** Compressibility for cubic  $\text{ZrMo}_2\text{O}_8$  up to 0.6 GPa (relative volume expansion is defined as  $100 \times [V_P - V_{\text{ambient}}]/V_{\text{ambient}}$ ). All of the data points were determined from neutron diffraction data. The straight line is a best fit to all of the data giving an average linear volume compressibility of  $2.24 \times 10^{-2} \text{ GPa}^{-1}$ .

diffraction experiments on cubic  $\text{ZrMo}_2\text{O}_8$  show no evidence for a phase transition in the temperature range 11–573 K. As shown in Figure 2, cubic  $\text{ZrMo}_2\text{O}_8$  undergoes negative linear isotropic thermal expansion over the entire temperature range ( $\alpha = -5.0 \times 10^{-6} \text{ K}^{-1}$ ). Additionally, the disordered structural model proposed for  $\beta\text{-ZrW}_2\text{O}_8$  in space group  $Pa\bar{3}$  gives a significantly better fit to all of our data than the  $\alpha\text{-ZrW}_2\text{O}_8$  model. This suggests that the disorder present in  $\beta\text{-ZrW}_2\text{O}_8$  and cubic  $\text{ZrMo}_2\text{O}_8$  may not be thermal in origin. Details of the structure analysis will appear in a subsequent paper. It should be noted that the linear thermal expansion coefficient for cubic  $\text{ZrMo}_2\text{O}_8$  is identical within experimental error to that observed for  $\beta\text{-ZrW}_2\text{O}_8$ .

Cubic  $\text{ZrMo}_2\text{O}_8$  ( $190.29 \text{ \AA}^3/\text{formula unit}$ ) shows no evidence for a phase transition below 0.6 GPa, analogous to the  $\alpha$  to  $\gamma$  transition reported by Evans and co-workers for cubic  $\text{ZrW}_2\text{O}_8$ ,<sup>6</sup> or a transformation to the more dense monoclinic ( $143.08 \text{ \AA}^3/\text{formula unit}$ ) or trigonal ( $173.82 \text{ \AA}^3/\text{formula unit}$ )  $\text{ZrMo}_2\text{O}_8$  structures. The average linear volume compressibility for cubic  $\text{ZrMo}_2\text{O}_8$  at room temperature is  $2.24 \times 10^{-2} \text{ GPa}^{-1}$

(21) Zhdanov, G. S.; Zhuravlev, N. N.; Stepanova, A. A.; Umanskiy, M. M. *Sov. Phys., Crystallogr.* **1957**, *2*, 284–285.

(22) Jorgensen, J. D.; Pei, S.; Lightfoot, P.; Hinks, D. G.; Veal, B. W.; Dabrowski, B.; Paulikas, A. P.; Kleb, R.; Brown, I. D. *Physica C* **1990**, *171*, 93–102.

below 0.6 GPa (see Figure 3). This value is more than 50% greater than that observed for  $\alpha$ -ZrW<sub>2</sub>O<sub>8</sub> ( $1.38 \times 10^{-2}$  GPa<sup>-1</sup>) and may be due to the different structures adopted by the two materials at room temperature.

While cubic ZrMo<sub>2</sub>O<sub>8</sub> (from 0 to ~660 K) exists over a narrower range of temperatures than cubic ZrW<sub>2</sub>O<sub>8</sub> (0–1050 and 1378–1530 K) its properties may offer advantages over ZrW<sub>2</sub>O<sub>8</sub>. In particular, the molybdate has a lower density than the tungstate, the lack of a discontinuity in thermal expansion at ~428 K may be important for some applications, and the absence of a low-pressure phase transition to a more dense structure

is of significance in the preparation of composite materials.

**Acknowledgment.** This research was supported by the National Science Foundation grant DMR-9623890. C.L. is grateful to the Georgia Rotary Student Program for a scholarship. The work at Argonne National Laboratory was supported by the U.S. Department of Energy, Division of Materials Sciences–Basic Energy Sciences under contract W-31-109-Eng-38.

CM980438M